GEOPHYSICAL RESEARCH LETTERS, VOL. 26, NO. 11, PAGES 1641-1644, JUNE 1, 1999

Testing plausible upper-mantle compositions using fine-scale models of the 410-km discontinuity

James B. Gaherty[1], Yanbin Wang[2], Thomas H. Jordan[3], and Donald J. Weidner[4]

Abstract. We constructed models of the 410-km discontinuity, in which the shape and width of the velocity and density increase were constrained by mineral physics data on the α–β transition in $(Mg,Fe)_2SiO_4$. The transition was represented as cubic functions of depth, and its width was estimated to range between 8-24 km. Reflection coefficients were calculated for these models for competing estimates of the percentage of olivine in the mantle, using synthetic seismograms that include the finite-frequency effects of the distributed transition. Comparing the synthetic reflectivities with the average reflectivity observed in previous analyses of *ScS* reverberations, we conclude that the mantle composition is close to that of pyrolite (55 vol. % olivine). Furthermore, much of the range of reflectivity can be explained by temperature variation in a pyrolite mantle. An olivine-poor composition (35 vol. % olivine) marginally satisfies the seismic data only if the transition thickness averages less than 10 km.

Introduction

The major seismic discontinuity at 410-km depth is widely accepted to be due to a solid-solid phase transition in the Earth's mantle. Experimental observations indicate that olivine transforms to wadsleyite (its β form) at the appropriate pressures and temperatures [e.g. *Katsura and Ito*, 1989]. To first order, the seismic properties of 410 match the experimental predictions for this transformation [e.g. *Ita and Stixrude*, 1992; *Vidale and Benz*, 1992]. In contrast, transitions in the other major mineral assemblages (e.g. eclogite to garnet) occur over broad pressure intervals, and thus cannot explain seismic reflections from 410-km depth [*Akaogi et al.*, 1987].

Because the 410 transition is restricted to the olivine system, the olivine content of the mantle can be estimated directly from the seismically determined magnitude of the 410-km discontinuity [e.g. *Bass and Anderson*, 1984; *Duffy and Anderson*, 1989; *Bina*, 1993; *Duffy et al.*, 1995]. In practice, this approach has proven inconclusive, however, primarily because the "data" in such analyses are not direct observations, but rather are models of seismic velocity and density, with associated uncertainties and assumptions. In particular, the 410 is usually represented as a discrete jump in velocity, or a linear velocity increase distributed over a few-kilometer depth interval. These assumptions are generally made to satisfy most simply a particular seismic data set, with little consideration given to mineralogical expectations, and they vary from study to study. It is therefore not surprising that this experiment has lead to few undisputed conclusions about upper-mantle composition and state.

We revisit this experiment using an analysis that more directly incorporates the constraints imposed by both seismic and mineral physics data. Our seismic data are shear-impedance contrasts for 410 previously determined for a broad region of the western Pacific and Asia. For representative mantle mineralogies, we constructed shear velocity and density profiles that included mineralogically realistic parameterizations of 410. We calculated synthetic reflectivities from these models using a technique analogous to that applied to the data. By comparing observed and predicted reflectivities, we determine the composition most consistent with seismological and mineralogical data.

Seismic Estimates of 410 Reflectivity

For our primary seismic datum on the observed magnitude of the 410-km discontinuity, we calculated the average reflection coefficient $R_0(410)$ and its standard deviation from the 31 regional values determined from *ScS* reverberations by *Revenaugh and Jordan* [1991] and *Revenaugh and Sipkin* [1994] (hereafter RJ91 and RS94, respectively). *ScS* reverberations include the ScS_n and $sScS_n$ phases (zeroth-order reverberations), as well as their primary reflections from upper-mantle discontinuities (first-order reverberations). RJ91 and RS94 determined travel times and amplitudes of the first-order reverberations for 31 source-to-receiver corridors via a stacking and migration procedure, providing a direct measure of shear reflectivity of the mantle in a variety of tectonic regions. The 31 regional values of $R_0(410)$ range from 0.7% to 6.7% (±1%), and yielded a mean value of 4.22% with a standard deviation of 1.24%. A large majority (25/31) of the values are clustered within ± one standard deviation of the mean; of the six outliers, two are low (0.7% and 2.8%), while four are bright (6.0-6.7%). In general, the observations are consistent with long-period shear-wave models [RJ91].

ScS reverberations are well suited to providing the mean and variance of 410 reflectivity because of the averaging inherent in the analysis. The 31 values reported by RJ91 and RS94 represent path averages of thousands of individual topside and bottom-side reflections from 410 in a wide range of tectonic regimes. Because the center frequencies of these waves were low (~25 mHz), the resulting estimates are less sensitive to small-scale lateral heterogeneity and boundary topography and more sensitive to finite-thickness (broad)

[1]School of Earth and Atmospheric Sciences, Georgia Institute of Technology, Atlanta
[2]Consortium for Advanced Radiation Sources, University of Chicago, Chicago, IL
[3]Department of Earth, Atmospheric, and Planetary Sciences, Massachusetts Institute of Technology, Cambridge
[4]CHiPR and Department of Geosciences, State University of New York, Stony Brook

Paper number 1999GL900312.
0094-8276/99/1999GL900312$05.00

transitions than those drawn from higher frequency waves such as *P'P'* and *P* coda. Perhaps most important for our purposes, the range of observed $R_o(410)$ were drawn directly from the data, rather than via seismic models of velocity and density. This simplified our evaluation of competing mineralogical models.

Mineralogical Models of 410

We started our mineralogical analysis with the α-olivine to wadsleyite phase-relation data of *Katsura and Ito* [1989], determined for $(Mg_{0.89}Fe_{0.11})_2Si0_4$ at 1473 K and 1873 K. Due to the unequal partitioning of iron between the α- and β-phases, the transformation occurs over a finite pressure interval, corresponding to a transition thickness of order 5-25 km. This width of this two-phase region depends on both temperature and bulk composition, with higher temperature and lower iron content corresponding to narrower widths. Furthermore, in this transition region, the growth of the β phase is generally non-linear in depth [e.g. *Stixrude*, 1997]. For mantle peridotites, the transformation starts slowly, with most of the β forming at the high-pressure end of the transition. Using the phase diagram for the transition and experimental thermoelasticity data assuming a typical mantle geotherm, we calculated the expected values of v_P, v_S, and density across the transition. We found that within the two-phase interval a physical property $X = v_P, v_S, \rho$ is well represented as a cubic function of depth z:

$$X(z) = X_0 + (\Delta X_1 - \tfrac{8}{3}\Delta X_2)\frac{(z-z_0)}{\Delta z} + \tfrac{8}{3}\Delta X_2\left(\frac{(z-z_0)}{\Delta z}\right)^3 \qquad (1)$$

for $z_0 < z < z_1$. In this expression, $\Delta X_1 = X(z_1) - X(z_0)$ is the total increase in $X(z)$ over the transition interval $z_0 < z < z_1 = z_0 + \Delta z$, and $\Delta X_2 = X_0 + \Delta X_1 - X(z_0 + \Delta z/2)$ is the deviation of $X(z)$ from linearity measured at the midpoint of the transition interval, $z_0 + \Delta z / 2$. The ratio $\Delta X_2 / \Delta X_1$ is well constrained by the experimental data to be about 0.13±.03 for all three properties, giving a shape similar to that analyzed by *Helffrich and Wood* [1996] and *Stixrude* [1997]. The exact value of $\Delta X_2 / \Delta X_1$ is actually not critical for our analysis, as low-frequency seismic waves are relatively insensitive to it. We fixed this parameter at the empirical value, and the form of 410 is specified by its thickness (Δz) and the total offset in properties (ΔX_1).

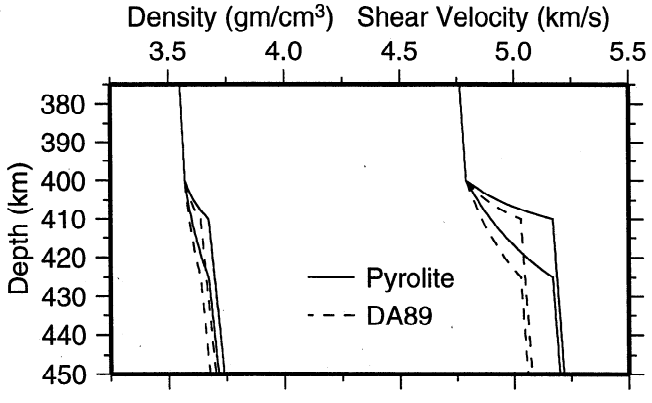

Figure 1. Density (left) and shear velocity (right) as a function of depth through the α-olivine to β-olivine phase transition. Solid lines represent pyrolite, while dashed lines correspond to DA89; Δz = 10 km and 24 km are shown for each. Total parameter contrasts used in calculating models (%): olivine, $\Delta v_S/v_S$=14.3±1.5, $\Delta\rho/\rho$=5.3±0.2; pyrolite, $\Delta v_S/v_S$= 7.9±0.9, $\Delta\rho/\rho$=2.9±0; DA89, $\Delta v_S/v_S$ =5.0±0.5, $\Delta\rho/\rho$ =1.9±0.1. The temperature derivative of the shear modulus for wadsleyite is taken to be −.014(4) GPa/K. Other properties from various sources, as summarized by *Weidner and Wang* [1999].

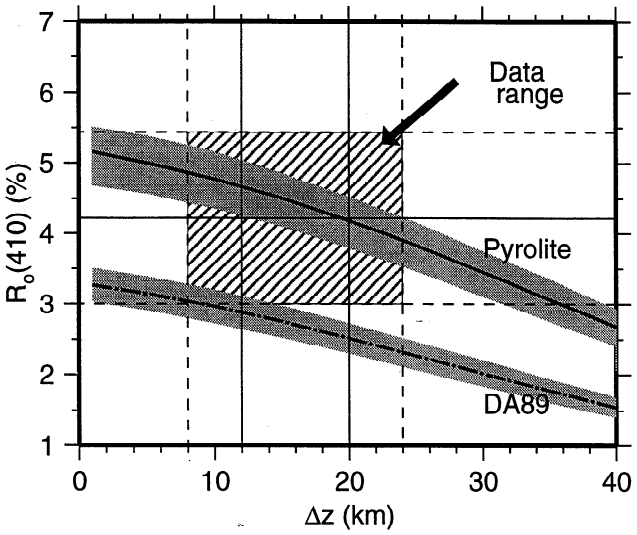

Figure 2. $R_o(410)$ computed from phase-transition models such as those in Fig. 1, plotted as a function of transition thickness Δz (curved lines with shaded bands). Curves for both pyrolite and DA89 are shown, and shading represents range of reflectivity due to uncertainties in the shear moduli, as listed in Table 1. Compositions are evaluated by comparing reflectivity curves with the target range of $R_o(410)$ and Δz (hatched box). Range of seismic observations (horizontal lines) is from RJ91 and RS94; the solid line represents the mean, while dashed lines represent ± one standard deviation. The best laboratory estimate of Δz is that it varies from 12-20 km (vertical solid lines), but uncertainties in various parameters result in a plausible thickness range of 8-24 km (vertical dashed lines).

Using equation 1 and the latest mineral physics estimates of elasticity and density (including variances) for the dominant mantle minerals, we calculated a suite of models for the 410-km discontinuity (Figure 1), where ΔX_1 and Δz are free parameters. The total offset ΔX_1 is controlled primarily by the amount of olivine in the mantle, relative to non-transforming phases such as pyroxene and garnet, and it is this parameter that we hope to constrain in our analysis. We chose as representative values the pyrolite model of *McDonough and Sun* [1994], which contains approximately 55% olivine by volume, and the more garnet-rich model of *Duffy and Anderson* [1989], with approximately 35 vol.% olivine (hereafter DA89).

The transition width Δz can be calculated from the phase diagram. *Katsura and Ito* [1989] estimated Δz as a function of temperature, with Δz = 19 km at 1673K, and Δz = 11 km at 2023K, ±6 km due to uncertainties in the pressure determination. Allowing for plausible variation in iron content (Mg# = 88-92) simply adds ±3 km uncertainty to these estimates.

We adjusted this estimated range of Δz to account for the effects of non-transforming phases such as garnet, and ortho- and clinopyroxene [*Stixrude*, 1997; *Irifune and Isshiki*, 1998]. Because Δz is dependent on the amount of iron in α and β, the presence of phases with greater or less affinity for iron can

impact the expected widths. Measured partition coefficients for iron [*Akaogi and Akimoto*, 1979; *Irifune and Isshiki*, 1998] imply that garnet has a strong narrowing effect on the transition, while pyroxene has a weaker effect. The abundance of garnet relative to pyroxene at 410-km depth is uncertain [e.g. *Ita and Stixrude*, 1992; *Irifune and Isshiki*, 1998], but assuming garnet is the dominant non-transforming phase, we calculated Δz of 8-15 km in the appropriate temperature range. A substantial amount of pyroxene at 410 will increase these widths by up to 4 km. These estimates correspond to pyrolite; for DA89, Δz decreases by 1-2 km due to reduced iron content in the α and β components.

This narrowing is partially offset by the increased geothermal gradient across the transition due to the positive Clapeyron slope [e.g. *Ita and Stixrude*, 1992]. We estimated that the ambient temperature increases by 60 K across the transition, which increases Δz by approximately 3 km. Our final estimates of 410 thickness for the probable range of temperatures in the mantle are displayed as the vertical band on Figure 2. The width ranges from 8 km at high temperature (1900 K), to 24 km at low temperature (1473 K). This range accounts for significant uncertainties in measured pressure, partition coefficients, and bulk composition; the "best-estimate" range is actually 12-20 km. Our width estimates are slightly wider than those estimated by *Stixrude* [1997] and *Irifune and Isshiki* [1998], primarily because they did not consider the thermal effect of the Clapeyron slope.

Testing Plausible Mantle Compositions

To model the average $R_0(410)$ estimate, we calculated synthetic vertical-incidence shear-wave reflections for a range of 410 parameterizations such as those shown in Figure 1. The calculation used a propagator-matrix technique (which included all finite-frequency effects) with a center frequency of 25 mHz and a passband of 15-45 mHz, similar to the data. Apparent reflection coefficients were estimated by cross-correlating the 410 model synthetic seismograms with synthetics calculated from a unit-amplitude step (first-order) discontinuity, analogous to the procedure of RJ91 and RS94. The resulting range of model $R_0(410)$ can be directly compared to the observations (Figure 2). Even for long-period waves such as these, the apparent reflection coefficient is dependent on the transition thickness Δz. Synthetic $R_0(410)$ approaches the actual total impedance contrast in both pyrolite and DA89 (5.23% and 3.38%, respectively) only for abrupt transitions. At a thickness of 20 km, the apparent reflectivity is down by over 20% in both cases.

Figure 2 indicates that either pyrolite or DA89 (marginally) provide an acceptable match to the observed $R_0(410)$, given the uncertainties in the seismic and mineralogical data. When the mineralogical expectation of transition thickness is considered, however, the data are most consistent with a mantle composition closer to pyrolite. DA89 approaches the observed mean reflectivity only for very narrow (0-10 km) transitions, and it seems unlikely that such widths are to be expected on average. In addition, it is impossible to explain brighter-than-average observations of 410 [e.g. RJ91; RS94; *Bostock*, 1996] with DA89, even using an abrupt transition and the most extreme mineralogical estimates for elasticity and density. Pyrolite matches the mean reflectivity with a transition width of 19 km. It can also explain much of the variance of $R_0(410)$ with transition widths ranging from 8 to 24 km, in good agreement with the thermally driven variations predicted by the mineralogical data.

Compositions other than pyrolite (55% olivine) also can satisfy our data within the uncertainties. Olivine contents as low as 45%, and as high as 65%, produce model $R_0(410)$ values within one standard deviation of the observed mean across the expected thickness range. The lower bound might be appropriate if the individual $R_0(410)$ of RJ91 and RS94 are consistently biased high, or if our thickness estimates are too large. The higher bound is preferred if the seismic observations are biased low, which might be expected due to topography on the transition [RJ91]. Taken at face value, however, the observations imply a composition close to pyrolite.

Discussion

Figure 2 implies that much of the variation of $R_0(410)$ observed by RJ91 and RS94 can be explained by temperature fluctuations in a pyrolite mantle, with little or no compositional heterogeneity required [*Bina and Helffrich*, 1994]. This arises because the reflective strength of 410 is dependent on transition thickness, which depends on temperature. The depth to 410 is also temperature dependent, and we hypothesize that the brightness of 410 should be positively correlated with its depth. Using the values cataloged by RJ91 and RS94 (eliminating one outlier), we find that depth and brightness are weakly correlated, with a linear coefficient of 0.28.

A pyrolite model with a thermally controlled transition thickness can potentially explain the range of reflectivities observed from higher-frequency reflected and/or converted arrivals [e.g. *Vidale and Benz*, 1993; *Bostock*, 1996; *Xu et al.*, 1998]. Observations of a "transparent" 410 are consistent with a broad (low-T) transition, while those requiring an apparently "sharp" 410 imply a relatively narrow (high-T) transition. Our ability to explain the latter is enhanced by the nonlinear models presented here, which are approximately a factor of two more reflective at frequencies above 0.2 Hz than a linear transition with the same total thickness (Figure 3). This

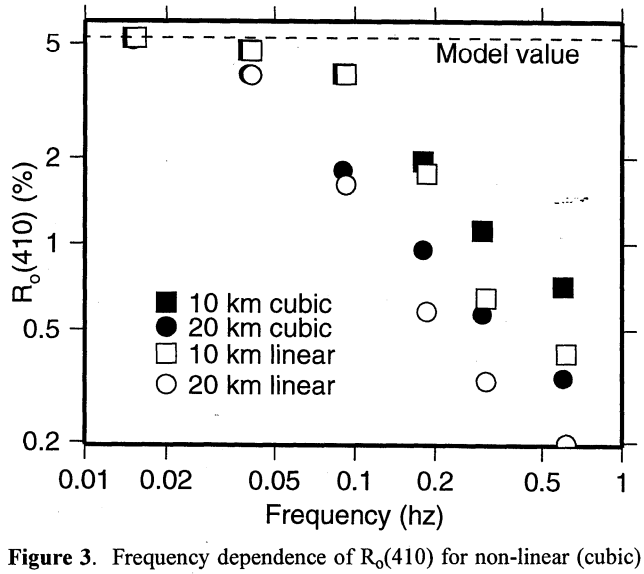

Figure 3. Frequency dependence of $R_0(410)$ for non-linear (cubic) transitions with 10-km and 20-km total thickness, and for comparable linear transitions with 10-km and 20-km thickness. Values of $R_0(410)$ are determined from synthetic seismograms in realistic finite-bandwidth windows.

conclusion is similar to that drawn by *Helffrich and Bina* [1994] and *Stixrude* [1997], while *Helffrich and Wood* [1996] argue that the variability in Δz (and thus reflectivity) is due to fluctuations in water content rather than temperature.

This thermal model probably cannot explain the anomalous observations of $R_0(410)$ that lie substantially outside the 1-σ band. These observations may reflect compositional variation, including heterogeneous olivine content, water content, and Mg #, among others. Wave propagation effects (e.g. focusing) are also a source of such anomalies.

It is important to reiterate that the fine-scale structure (shape and thickness) built into our models of 410 were not determined from seismic data. Rather, we employed information from mineral physics to construct a plausible range of models with which to work, and used the seismic data only to test compositional models. Theoretically, seismic data can provide independent, localized estimates of 410 thickness by considering the frequency dependence of the response (Figure 3); the amplitude should fall off with frequency, and the apparent depth of the reflector (as inferred from the travel time) should increase [*Helffrich and Bina*, 1994]. Observations of 410 reflectivity as a function of frequency are generally consistent with a distributed transition [e.g. *Bostock*, 1996; *Xu et al.*, 1998]. In a particularly interesting study, *Melbourne and Helmberger* [1998] analyzed the frequency-dependence of 410 triplications beneath the western US. They proposed a *P*-velocity model of 410 that is nearly identical to those shown in Figure 1; the discontinuity is represented by a transition that starts slowly, ends abruptly, and has a thickness of ~25 km.

Acknowledgments. We thank C. Bina and an anonymous referee for useful reviews. Figures were generated using GMT [*Wessel and Smith*, 1995]. This research was supported by NSF Grants EAR-9709905 (Jordan) and EAR-9709996 (Weidner) under the CSEDI (Cooperative Studies of the Earth's Deep Interior) program.

References

Akaogi, M. and S. Akimoto, High-pressure phase equilibria in a garnet lherzolite, with special reference to Mg^{2+}–Fe^{2+} partitioning among constituent minerals, *Phys. Earth Planet. Int., 19*, 31-51, 1979.

Akaogi, M., A. Navrotsky, T. Yagi, and S. Akimoto, Pyroxene-garnet transformation: Thermochemistry and elasticity of garnet solid solutions, and application to a pyrolite mantle, in High-Pressure Research in Mineral Physics, ed. M.H. Manghnani and Y. Syono, pp. 251-260, Terra Scientific, Tokyo,1987.

Bass, J.D. and D.L. Anderson, Composition of the upper mantle: Geophysical tests of two petrological models, *Geophys. Res. Lett., 11*, 237-240, 1984.

Bina, C. R., Mutually consistent estimates of upper mantle composition from seismic velocity contrasts at 400 km depth, *Pure Appl. Geophys., 141*,101-109, 1993

Bina, C. R., and G. Helffrich, Phase transition Clapeyron slopes and transition zone seismic discontinuity topography, *J. Geophys. Res., 99*, 15,853-15,860, 1994.

Bostock, M.G., A seismic image of the upper mantle beneath North American craton, *Geophys. Res. Lett., 23*, 1593-1596, 1996.

Duffy, T.S. and D.L. Anderson, Seismic velocities in mantle minerals and the mineralogy of the upper mantle, *J. Geophys. Res., 94*, 1895-1912, 1989.

Duffy, T.S., C.S. Zha, R.T. Downs, H.K. Mao, and R.J. Hemley, Elasticity of forsterite to 16 Gpa and the composition of the upper mantle, *Nature, 378*, 170-173, 1995.

Helffrich, G. and Bina, C.R., Frequency dependence of the visibility and depths of mantle seismic discontinuities, *Geophys. Res. Lett., 21*, 2613-2626, 1994.

Helffrich, G. and Wood, B.J., 410-km discontinuity sharpness and the form of the olivine α–β phase diagram--resolution of apparent seismic contradictions, *Geophys. J. Int., 126*, F7-F12, 1996.

Irifune, T. and M. Isshiki, Iron partitioning in a pyrolite mantle and nature of the 410 km seismic discontinuity, *Nature, 392*, 702-705, 1998.

Ita, J. and L. Stixrude, Petrology, elasticity, and composition of the mantle transition zone, *J. Geophys. Res., 97*, 6849-6866, 1992.

Katsura, T. and E. Ito, The system Mg_2SiO_4-Fe_2SiO_4 at high pressures and temperatures: Precise determination of stabilities of olivine, modified spinel, and spinel, *J. Geophys. Res., 94*, 15,663-15,670, 1989.

McDonough, W.F. and S.-S. Sun, The composition of the Earth, *Chem. Geol., 120*, 223-253, 1995.

Melbourne, T. and D. Helmberger, Fine structure of the 410 km discontinuity, *J. Geophys. Res., 103*, 10,091-10,102, 1998.

Revenaugh, J.S. and T.H. Jordan, Mantle layering from *ScS* reverberations, 2, The transition zone, *J. Geophys. Res., 96*, 19,763-19,780, 1991.

Revenaugh, J.S. and S.A. Sipkin, Mantle discontinuity structure beneath China, *J. Geophys. Res., 99*, 21,911-21,928, 1994.

Stixrude, L., Structure and sharpness of phase transitions and mantle discontinuities, *J. Geophys. Res., 102*, 14,835-14,852, 1997.

Vidale, J.E. and H.M. Benz, Upper-mantle seismic discontinuities and the thermal structure of subduction zones, *Nature, 365*, 678-683, 1992.

Weidner, D.J. and Y. Wang, Phase transformations: Implications for mantle structure, in *Mineral Physics and Seismic Tomography, Geophys. Monograph*, S. Karato, G. Masters, L. Stixrude, R.C. Liebermann, and A.M. Forte, eds., in press, 1999.

Wessel, P. and W.H.F. Smith, New version of Generic Mapping Tools released, *Eos, 76*, 329, 1995.

Xu, F., J.E. Vidale, P.S. Earle, and H.M. Benz, Mantle discontinuities under southern Africa from precursors to *P'P'df*, *Geophys. Res. Lett., 25*, 571-574, 1998.

J.B. Gaherty, School of Earth and Atmospheric Sciences, Georgia Institute of Technology, Atlanta, GA 30332-0340 (email: gaherty@eas.gatech.edu)

T.H. Jordan, Dept. of Earth, Atmospheric, and Planetary Sciences, Bldg. 54-526, MIT, Cambridge, MA 02139

Y. Wang, Consortium for Advanced Radiation Sources, University of Chicago, 5640 S. Ellis Ave, Chicago, IL 60637

D.J. Weidner, CHiPR and Dept. of Geosciences, State University of New York, Stony Brook, NY 11794

(Received February 16, 1999; revised April 1, 1999;
accepted April 16, 1999.